ARTICLES

Solution Properties of Urea and Its Derivatives in Water: Evidence from Ultrasonic Relaxation Spectra

A. Rupprecht and U. Kaatze*

Drittes Physikalisches Institut, Georg-August-Universität, Bürgerstrasse 42-44, 37073 Göttingen, Germany

Received: February 1, 2002; In Final Form: May 21, 2002

Between 200 kHz and 4.6 GHz, ultrasonic absorption spectra of aqueous solutions of urea and some of its alkyl derivatives have been measured at various solute concentrations. The derivatives comprise methylurea, ethylurea, *N*-propylurea, tetramethylurea, *N*,*N*-diethylurea, *N*,*N*′-diethylurea, and *N*-butylurea. Up to very high concentrations of the solute, solutions of urea do not show noticeable contributions from relaxation processes in their absorption spectra. Depending upon concentration, the solutions of the alkyl derivatives reveal absorption in excess of the asymptotic high-frequency part of the spectra. This excess absorption is discussed in terms of a recent unifying model of noncritical concentration fluctuations. Parameters of this model, particularly the fluctuation correlation length and the relaxation rate on the order of parameter fluctuations, reflect in an obvious manner the hydrophobic character of the solutes. Comparison with other series of aqueous solutions exhibiting precritical behavior clearly shows the hydrophilic part of solute molecules to be of low significance in determining the maximum fluctuation correlation length of the liquids. Rather, the number and steric arrangement of carbohydrate groups are the dominant factors that cause noncritical local fluctuations in the concentration of solutes.

1. Introduction

The solution behavior of urea is of considerable significance in biophysics. Urea serves as an effective protein denaturant, and almost all of the amino groups from surplus amino acid that is not required for the synthesis of proteins or other biomolecules are converted to urea. Despite its prominent role in biology, urea continues to intrigue and fascinate solution chemists because of the curious manner in which it affects aqueous solutions. "Urea is considered a solute class of its own, because of the possibly unique characteristics of its interactions with water."[1] For this reason and also in liquid-state physics, much interest is directed toward the properties of urea/water systems.

In attempting to explain the concentration dependence of thermodynamic parameters of aqueous solutions of urea, Stokes has proposed an association model[2] in which urea molecules, according to an isodesmic reaction scheme

$$U_n + U_1 \underset{k_{rn}}{\overset{k_{fn}}{\rightleftharpoons}} U_{n+1} \qquad n = 1, 2, \cdots \tag{1}$$

form clusters U_{n+1} from monomers U_1. Frank and Franks, also dealing with the thermodynamic properties of urea in solution, employed a different model.[3] Assuming water to consist of a dense non-hydrogen-bonded phase $(H_2O)_d$ and a tetrahedrally H-bonded bulky phase $(H_2O)_b$, they considered urea to mix ideally with $(H_2O)_d$ but not to interact with the bulky clusters $(H_2O)_b$. This model predicts urea to promote structure-breaking effects because of a shift, in favor of the dense phase, of the equilibrium between the dense and the bulky water. Hence, within the framework of this model, the effect of urea in solution may be described by catalytic action in the dense−bulky phase equilibrium:

$$(H_2O)_b + U \underset{k_r}{\overset{k_f}{\rightleftharpoons}} (H_2O)_d + U \tag{2}$$

Ultrasonic spectrometry up to frequencies of 800 MHz did not show evidence of either of the equilibria (eqs 1 and 2) in aqueous urea solutions.[4−6] However, the Frank and Franks model may be taken to be supported by NMR results,[7] which have also been discussed in terms of the destruction of long-range order characteristics of the water hydrogen network by urea. Another experimental result is the missing frequency shifts or shape alterations in the relevant H-bond Raman line on addition of urea to water.[8] This finding has been taken to support the conclusion that this particular solute does not affect the nature of the water−water hydrogen bonds but that it tends to diminish the degree of H-bonding.

A different view has been obtained from dielectric spectrometry,[9] which, on one hand, revealed a urea hydration water relaxation time τ_h larger than the dielectric relaxation time of water ($\tau_h \approx 2\tau_w$, $c \leq 2$ M, 25 °C) but, on the other hand, showed an unusually small number Z_h of affected ("hydration") water molecules per molecule of urea ($2.6 \leq Z_h \leq 4.3$). These findings may be considered in light of modern ideas of the dielectric relaxation of associating liquids.[10,11]

On the basis of computer simulation studies of water,[12−16] these ideas lead to a molecular dynamics model in which the

* Corresponding author. E-mail: uka@physik3.gwdg.de.

10.1021/jp020322k CCC: $22.00
Published on Web 08/21/2002

TABLE 1: Formula, Shorthand Notations, and Purity of Solutes

urea	NH_2CONH_2	U	99.5%
methylurea	$CH_3NHCONH_2$	MeU	97%
ethylurea	$C_2H_5NHCONH_2$	EtU	98%
N-propylurea	$C_3H_7NHCONH_2$	*N*-PrU	98%
tetramethylurea	$(CH_3)_2NCON(CH_3)_2$	$(Me)_4U$	99%
N,*N*-diethylurea	$(C_2H_5)_2NCONH_2$	*N*,*N*-$(Et)_2U$	97%
N,*N*′-diethylurea	$C_2H_5NHCONHC_2H_5$	*N*,*N*′-$(Et)_2U$	97%
N-butylurea	$C_4H_9NHCONH_2$	*N*-BuU	99%

local concentration of hydrogen-bonding groups or molecules plays a dominant role.[17,18] If this view is accepted, the solution behavior of urea in water should be noticeably affected by hydrophobic groups attached to the hydrophilic molecules. Because aqueous solutions of urea did not reveal indications of acoustical excess absorption,[4−6] measuring ultrasonic absorption over a wide frequency range is likely a sensitive method to investigate the effects from additional hydrophobic groups attached to the urea molecule. We therefore performed a broadband ultrasonic spectrometry study of aqueous solutions of urea and some of its alkyl derivatives.

2. Experimental Section

Urea Derivatives and Their Solutions. It is the aim of this study to contribute to a better understanding of the effect of hydrophobic groups attached to urea on the structure and of molecular dynamics in water. We therefore focus first on the series of *n*-alkyl derivatives from urea to *N*-butylurea. To look for particular influences on the solution properties resulting from the steric arrangement of alkyl groups, tetramethylurea, *N*,*N*-dielethylurea, and *N*,*N*′-diethylurea are also included for comparison with *N*-butylurea. A survey of the solutes is given in Table 1 along with shorthand notations that will be used in this paper.

Because we expect small effects in the ultrasonic absorption coefficient of aqueous systems from the hydration of urea and its derivatives, we studied solutions of all solutes at the rather high solute concentration of $c = 1$ M. On one hand, this concentration is considered still sufficiently small to avoid intolerable overlaps of hydration regions, and on the other hand, it is high enough for there to be significant effects in the broadband spectra from the molecular mechanisms under study. For some solutes, the validity of these assumptions has been inspected by also considering solutions at different concentrations. In a previous ultrasonic study,[19] an attempt has been made to relate the excess absorption spectra to noncritical local fluctuations in the concentration of the binary liquid. Because such fluctuations are expected to become especially obvious at high solute content, we also conducted some measurements at very high solute concentrations up to 10.5 M.

Sample liquids were prepared by weighing appropriate amounts of the solute into suitable flasks, which afterward were filled up to the line measure with bidistilled and additionally deionized water. The solutes with purity between 97 and 99.5% (Table 1) were supplied by Fluka, Aldrich, and Alfa and were used without additional purification. The density ρ and shear viscosity η_s of the solutions were measured pycnometrically and with the aid of a falling-ball viscometer (type B/BH, Haake, Karlsruhe, Germany), respectively. Concentration data as well as the density and shear viscosity values of the aqueous solutions are given in Table 2.

Ultrasonic Absorption Spectrometry. The ultrasonic absorption coefficient α of liquids at frequency ν is normally

TABLE 2: Molar Concentration *c*, Mass Fraction *Y*, Molality *m*, and Mole Fraction *x* of Solute as Well as Density ρ, Shear Viscosity η_s, and Sound Velocity c_s at Approximately 1 MHz of the Solutions at 25 °C

c, M ±0.2%	*Y* ±0.1%	*m*, mol/kg ±0.1%	*x* ±0.1%	ρ, g/cm^3 ±0.1%	η_s, 10^{-3} Pa s ±2%	c_s, m/s ±0.1%
			U			
1.01	0.060	1.06	0.0188	1.014	0.934	1518.9
9.06	0.481	15.4	0.217	1.133	1.59	1705.7
			MeU			
1.01	0.074	1.08	0.0191	1.009	1.02	1533.1
10.5	0.696	30.8	0.357	1.116	5.92	1750.5
			EtU			
1.00	0.088	1.09	0.0193	1.007	1.10	1548.6
4.16	0.352	6.18	0.100	1.039	2.24	1671.6
7.00	0.581	15.7	0.221	1.062	4.98	1702.6
8.71	0.716	28.6	0.340	1.072	8.17	1698.4
			N-PrU			
1.00	0.101	1.10	0.0195	1.005	1.20	1562.2
2.03	0.204	2.51	0.0433	1.015	1.59	1616.5
2.97	0.296	4.12	0.0691	1.023	2.34	1644.3
3.92	0.389	6.24	0.1010	1.030	2.94	1651.6
			$(Me)_4U$			
1.00	0.117	1.14	0.0201	0.999	1.31	1566.3
2.21	0.256	2.96	0.0506	1.004	2.07	1632.2
3.02	0.349	4.61	0.0766	1.008	2.66	1655.6
5.06	0.581	11.9	0.177	1.011	4.38	1661.7
5.78	0.666	17.1	0.236	1.009	4.87	1637.6
6.96	0.811	37.0	0.400	0.997	3.91	1561.6
8.28	1.000		1.00	0.962	1.40	1396.5
			N,*N*-$(Et)_2U$			
1.00	0.116	1.13	0.0200	1.003	1.35	1574.0
1.70	0.195	2.08	0.0361	1.017	1.63	1619.8
1.91	0.218	2.40	0.0414	1.020	1.75	1630.3
			N,*N*′-$(Et)_2U$			
1.00	0.116	1.13	0.0200	1.001	1.39	1574.4
1.68	0.195	2.08	0.0361	1.005	1.86	1619.8
1.89	0.218	2.40	0.0414	1.006	2.03	1629.9
			N-BuU			
0.500	0.058	0.531	0.0095	1.000	1.07	1537.8
0.802	0.093	0.882	0.0156	1.002	1.20	1558.2
0.902	0.105	1.01	0.0178	1.002	1.24	1566.1
1.00	0.116	1.13	0.0199	1.003	1.28	1569.8
1.09	0.127	1.25	0.0220	1.003	1.30	1573.7
1.15	0.134	1.33	0.0234	1.004	1.35	1577.0
1.26	0.145	1.46	0.0257	1.005	1.42	1579.4

expressed by two terms:

$$\alpha(\nu) = B^{|}\nu^2 + \alpha_{exc}(\nu) \qquad (3)$$

Herein, $B^{|}\nu^2$ denotes a high-frequency background contribution to α, with $B^{|}$ independent of ν. α_{exc} is the frequency-dependent excess part in α in which we are mainly interested in spectrometry. Because of the strong frequency dependence of the background contribution, which is quadratic in ν, the sonic absorption coefficient varies by more than a factor of 10^9 within the frequency range of the measurements (0.2 MHz $\leq \nu \leq$ 4600 MHz). To account for this large range of α values appropriately, two different methods of measurement and altogether six different specimen cells, each matched to a special frequency range, have been used. At frequencies below 15 MHz, a cavity resonator method was applied in which the effective path length of interaction of the acoustical field with relevant modes within the sample liquids was substantially increased by multiple reflections of the sonic signal.[20,21] Using this method, we performed quality factor measurements in which the attenuation

coefficient α is determined relative to a sound velocity and the acoustical impedance is matched to that of a reference liquid with a well-known absorption coefficient. We used methanol/water mixtures as well as aqueous solutions of sodium chloride and of urea as references. The latter do not exhibit any indication of excess absorption at sufficiently low urea concentration ($c < 5$ M), so their $B^{|}$ values (eq 3) have been determined by absolute α measurements at higher frequencies (see below). We used two different resonator cells. A plano-concave cell[22] (diameter $d = 70$ mm, length $l = 19$ mm), with a radius of curvature $R_c = 2$ m of one face, was designed for measurements at low frequencies ($\nu \leq 2.8$ MHz). A biplanar[23] cell ($d = 16.8$ mm, $l = 6$ mm) was suitable at higher frequencies (1 MHz $\leq \nu \leq$ 15 MHz). To consider higher-order "satellite" modes carefully, the complete transfer function of the resonator was always recorded continuously in a reasonable frequency range using a network analyzer setup, and suitable analytical expressions were fitted to a piece of the transfer function to extract the undisturbed principal resonance peak. In doing so, small effects from electrical crosstalk and also from differences between the α values of the sample and the reference liquid[24] have been taken into account.

In the frequency range from 3 to 4.6 MHz, absolute α measurements have been performed using a pulse-modulated sonic-wave transmission method at variable sample length.[20,21] We employed four cells that mainly differ from one another by their dimensions and piezoelectric transmitter and receiver units. At 3 MHz $\leq \nu \leq$ 63 MHz, a cell[25] was utilized in which quartz transducer disks were operated at odd overtones of their fundamental frequency ν_T of thickness vibrations ($\nu_T = 1$ MHz, $d = 40$ mm). At 30 MHz $\leq \nu \leq$ 530 MHz, lithium niobate transducer disks [26] ($\nu_T = 10.8$ MHz, $d = 12$ mm) were excited at frequencies $\nu_T(2n + 1)$ in which $n = 1, 2, \ldots$. Between 500 MHz and 2 GHz, broadband end-face excitation of lithium niobate rods[27] ($d = 3$ mm, $l_T = 10$ mm), according to the principle of Bömmel and Dransfeld,[28] was applied. Finally, in the frequency range between 1.1 and 4.6 GHz, the transducers were thin ZnO films ($\nu_T = 1.3$ GHz, $d = 2$ mm) sputtered onto delay lines made of sapphire[27] and were again operated in modes of thickness vibration. At each frequency of measurement, the transfer function of the cell has been determined at 400 transducer spacings. The transfer characteristics of the electronic apparatus have been routinely recorded in runs in which the signal passed a high-precision below-cutoff piston attenuator[29] instead of a cell. To account for possible effects from diffraction due to the finite transducer diameter, a semiempirical correction based on reference measurements with liquids of well-known attenuation coefficients has been applied at low frequencies.

Sound Velocity. The sound velocity c_s of the samples was required for proper matching of the reference liquids in the cavity resonator measurements and also for the presentation of the absorption spectra in the common form

$$(\alpha\lambda)_{exc} = \alpha c_s/\nu - B^{|}c_s\nu = \alpha c_s/\nu - B\nu \qquad (4)$$

where $\lambda = c_s/\nu$ and $B = B^{|}c_s$. The sound velocity has been determined at 0.2 MHz $\leq \nu \leq$ 15 MHz from the frequencies of successive principal cell resonance peaks, taking into account the nonequidistancy of the resonance frequencies.[20] At high frequencies, additional c_s values were available from the waviness in the cell transfer function due to multiple reflections of the acoustical signal at small transducer spacings l.

Experimental Accuracy. Fluctuations in the frequencies of measurements were negligibly small. The temperature of the sample cells was controlled to within 0.03 K, and it was measured with an accuracy of 0.02 K. Temperature gradients and differences in the temperature of different cells did not exceed 0.05 K, corresponding to an estimated error of less than 0.1% in absorption coefficient data. A careful analysis of the other sources of possible error shows that the accuracy of the α measurements depends on the properties of the samples. Globally, the accuracy of the measurements can be characterized by an experimental error of $\Delta\alpha/\alpha = 0.04$ in the data resulting from the resonator quality-factor measurements. If $\alpha/\nu^2 < 50 \times 10^{15}$ m^{-1}s^2, the error may be higher in some parts of that frequency band but does not exceed $\Delta\alpha/\alpha = 0.1$. For the absorption coefficient data from pulse-modulated wave transmission measurements, $\Delta\alpha/\alpha = 0.02$ at 3 MHz $\leq \nu \leq$ 30 MHz, $\Delta\alpha/\alpha = 0.005$ at 30 MHz $\leq \nu \leq$ 300 MHz, and $\Delta\alpha/\alpha = 0.01$ at 300 MHz $\leq \nu \leq$ 4600 MHz. The error in the sound velocity is $\Delta c_s/c_s = 0.001$ at 3 MHz $> \nu >$ 500 MHz, and it is $\Delta c_s/c_s = 0.0005$ at 3 MHz $\leq \nu \leq$ 500 MHz.

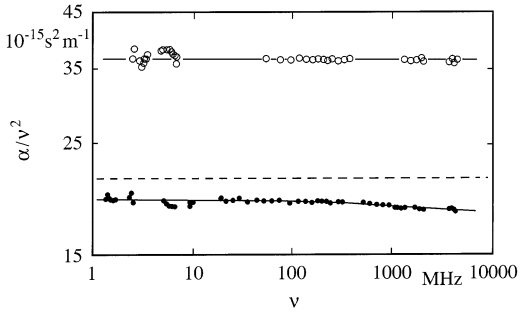

Figure 1. Ultrasonic absorption spectra in the form of α/ν^2 vs ν for a 9.06 M solution of urea in water (●) and for $(Me)_4U$ (○) at 25 °C. Solid lines are drawn to indicate the trends in the data. The dashed line shows the frequency-independent α/ν^2 value of water at the same temperature.

3. Results

In Figure 1, the ultrasonic absorption coefficients per ν^2 data of $(Me)_4U$ without water added are shown as a function of frequency ν. The frequency-normalized spectrum, like that of water, which is indicated by the dashed line in Figure 1, is constant within the complete range of measurement:

$$\alpha/\nu^2 = B^{|} \qquad (5)$$

Obviously, no relaxation process exists in pure tetramethylurea within the frequency range under consideration. Also displayed in Figure 1 are the α/ν^2 data for the 9.1 M solution of urea in water. A small dispersion ($d(\alpha/\nu^2)/d\nu < 0$) in the data can just be resolved, indicating a low amplitude relaxation process at high frequencies.

In Figure 2, for solutions of *N*-PrU in water, this relaxation region is presented in the form of $(\alpha\lambda)_{exc}$ versus ν, by which the high-frequency region of the spectrum is accentuated. As evident from the spectra, the maximum value $(\alpha\lambda)_{exc}(\hat{\nu})$ of the excess absorption per wavelength increases with c, whereas at $c \leq 3$ M, the frequency $\hat{\nu}$ of the maximum decreases. Toward high concentration, deviations from the shape of a simple Debye-type relaxation spectrum

$$(\alpha\lambda)_{exc} = \frac{A\omega\tau}{1 + \omega^2\tau^2} \qquad (6)$$

governed by a discrete relaxation time τ, emerge. In eq 6, A denotes the relaxation amplitude ($(\alpha\lambda)_{exc}(\hat{\nu}) = A/2$, $\hat{\nu} = (2\pi\tau)^{-1}$), and $\omega = 2\pi\nu$ is the angular frequency. Such deviations from

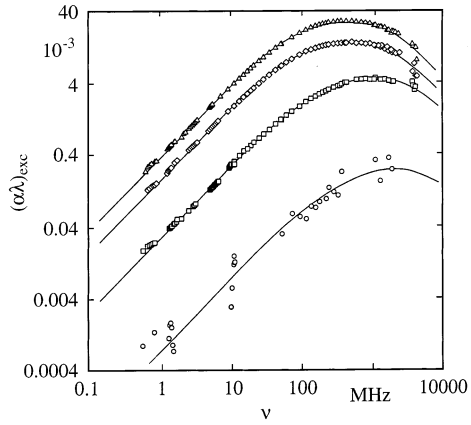

Figure 2. Ultrasonic excess absorption per wavelength plotted as a function of frequency ν for solutions of *N*-PrU at 25°C: ○, 1 M; □, 2.03 M; ◇, 2.97 M; △, 3.92 M. The curves are graphs of the relaxation spectral function defined by eq 13 with the parameter values given in Table 3.

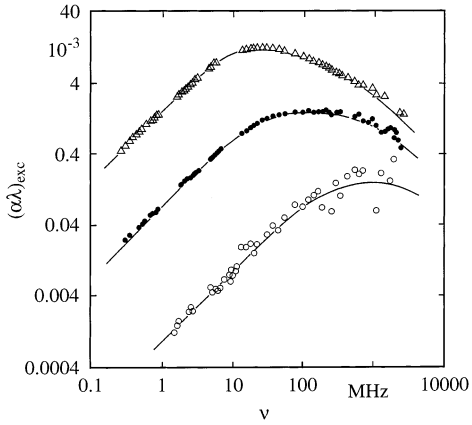

Figure 3. Ultrasonic excess absorption spectra for aqueous solutions of *N*-BuU at 25 °C: ○, 0.5 M; ●, 0.9 M; △, 1.26 M. The curves represent the $R_{um}(\nu)$ function (eq 13) with the parameter values found in the fitting procedures (Table 3).

the graph of a Debye relaxation term (eq 6) are even more obvious in the spectra of *N*-BuU solutions, some examples of which are presented in Figure 3. Again, the maximum excess absorption increases with solute concentration, and the frequency $\hat{\nu}$ of the maximum absorption decreases. This latter finding is a strong indication that the underlying relaxation may not be due to a simple elementary reaction. Particularly for the isodesmic reaction scheme shown in eq 1 and the catalytic reaction displayed in eq 2, the relaxation rate τ^{-1} corresponding to $2\pi\hat{\nu}$ is predicted[30] to increase with concentration c.

4. Discussion

Concentration Fluctuation Model. The concentration dependence of the frequency $\hat{\nu}$ of maximum absorption per previously discussed spectrum suggests that noncritical fluctuations in the local concentration give rise to the acoustical absorption rather than a stoichiometrically defined elementary reaction. The characteristic relaxation rate of such fluctuations is given by[31]

$$\tau_\xi^{-1} = 2D/\xi^2 \tag{7}$$

where D denotes the mutual diffusion coefficient and ξ the fluctuation correlation length. If spatial correlations in the fluctuations are assumed to follow an Ornstein−Zernike ansatz,[32,33] the Kawasaki−Ferrell[34,35] equation

$$D = k_B T/(6\pi\eta_s\xi) \tag{8}$$

relates ξ to D. Using this relation,

$$\tau_\xi^{-1} = k_B T/(3\pi\eta_s\xi^3) \tag{9}$$

follows from eq 7, showing that τ_ξ^{-1} substantially decreases with increasing fluctuation correlation length. Hence, our finding that $\hat{\nu}$ decreases with c may be taken as an indication that ξ increases with the concentration of urea derivatives.

A careful analysis of the measured spectra shows that some of the slopes are incompatible with the original Romanov−Solov'ev concentration fluctuation theory.[36−39] However, the complete set of spectra is consistent with the unifying model of noncritical concentration fluctuations,[40] which combines aspects of various previous theories.[41−43] In this model, only long-range spatial correlations are assumed to follow Ornstein−Zernike behavior, as suggested by Endo[42] and Kühnel et al.,[43] whereas short-range correlations, following Montrose and Litovitz,[41] are considered by a nearly exponential decay. This assumption leads to the weight function

$$\hat{f}(q) \propto (1 + 0.164(q\xi) + 0.25(q\xi)^2)^{-2} \tag{10}$$

in the autocorrelation function of order parameter fluctuations

$$\phi(q, t) = \hat{f}(q)\exp(-t/\tau_g) \tag{11}$$

in q space. Here, $q = |\vec{q}|$ is the value of the wave vector, and the order parameter is the difference in the local concentration from the mean. The relaxation time τ_g is given by the relation

$$\tau_g^{-1} = Dq^2 + \tau_o^{-1} \tag{12}$$

where τ_o is the relaxation time of a rate process that, in parallel to diffusion, controls the time behavior of the fluctuations. Because of the choice of the special weight function $\hat{f}(q)$ (eq 10), the relaxation spectral function

$$R_{um}(\nu) = Q\int_0^\infty \hat{f}(q)\frac{\omega\tau_g}{1+\omega^2\tau_g^2}q^2\,dq \tag{13}$$

describing the response of the liquid to compressional wave exposure can be integrated without introducing artificial limits. In the $R_{um}(\nu)$ function, Q is an amplitude factor assumed from the sum of the amplitude factor Q_{RS} of the Romanov−Solo'ev model and the Montrose−Litovitz contribution Q_{ML} resulting from a shear viscosity relaxation with identical frequency behavior.

Equation 13 has been fit to the experimental spectra. The values for the parameters Q, D, and τ_o that followed thereby are collected in Table 3, along with the fluctuation correlation length ξ resulting from eq 8. Also given is the relaxation time $\hat{\tau} = (2\pi\hat{\nu})^{-1}$ corresponding to the frequency $\hat{\nu}$ of the maximum in the excess absorption spectra.

Relaxation-Time Distribution Function. Physical aspects of the relaxation spectral function $R_{um}(\nu)$ (eq 13) are more easily extracted from the corresponding relaxation-time distribution function $G_{um}(r)$, defined by

$$R_{um}(\nu) = Q\int_0^\infty G_{um}(r)\frac{\omega\tau}{1+\omega^2\tau^2}\,dr \tag{14}$$

TABLE 3: Parameters of the Relaxation Spectral Function $R_{um}(\nu)$ (eq 13), B Value of the Asymptotic High Frequency Contribution to the Spectra and Empirical Relaxation Time $\hat{\tau}$ Corresponding with the Maximum in the Excess Absorption Spectra for Solutions at 25 °C[a]

c, M	Q, 10^{-30} m^3 ±5%	D^{-10} m^2 s^{-1} ±5%	ξ, 10^{-10} m ±5%	τ_o, ns ±10%	B, ps ±0.5%	$\hat{\tau}$, ps ±1%
			U			
1.01					30.8	
9.06	0.04	8	1.8		30.9	27
			MeU			
1.01					32.1	
10.5	1.4	17	0.2		51	10
			EtU			
1.00	0.04	8	2.5		32.2	28
4.16	0.37	3.7	2.6		40.3	62
7.00	0.73	2.5	1.7		56.8	79
8.71	0.77	2.2	1.2		84.4	85
			N-PrU			
1.00	0.03	4	4.5	5	32.2	78
2.03	0.75	2.5	5.5	6.8	37.2	146
2.97	3.93	1.4	6.7	7.4	42.3	320
3.92	6.26	1.2	6.2	7.9	48.1	338
			$(Me)_4U$			
1.00	0.18	8	2.1		32.9	26
2.21	0.19	7	1.5		40.1	28
3.02	0.46	6.3	1.3		41.0	30
5.06	0.83	4	1.2		53.3	46
5.78	0.82	4	1.1		53.7	46
6.96	0.64	5.6	1.0		56.0	38
8.28					51.0	
			N,*N*-$(Et)_2$U			
1.00	0.13	7	2.3		33.9	31
1.70	0.26	5.8	2.3		36.3	38
1.91	0.35	5.7	2.2		36.6	37
			N,*N*′-$(Et)_2$U			
1.00	0.13	4.1	3.9		36.2	69
1.68	0.41	2.8	4.1		40.7	104
1.89	0.83	2.1	5.2		42.7	167
			N-BuU			
0.50	0.05	2.9	7.0	2.7	33.2	160
0.80	0.93	1.6	11.2	10	34.3	550
0.90	4.09	1.2	15.1	16	34.6	1260
1.00	17.9	0.8	20.3	18.7	35.3	2980
1.09	52	0.7	23.8	20	35.9	4500
1.15	101	0.6	27.0	20.6	36.1	6060
1.26	205	0.5	29.8	19.8	36.2	7260

[a] For the solutions with high frequency and small amplitude relaxation terms, the errors in the parameter values may be larger.

with the normalization relation

$$\int_0^\infty G_{um}(r)\,dr = 1 \qquad (15)$$

In these equations, $r = \ln(\tau/\tau^*)$ where r^* denotes a suitably chosen reference relaxation time. Here, we will use $\tau^* = 1$ ns. For the unifying model of concentration fluctuations, the relaxation-time distribution function can be given in analytical form.[40] In Figure 4, $G(r)$ is displayed for some solutions of urea derivatives using the parameters of Table 3.

The relaxation-time distribution of the $(Me)_4U$ solution exhibits an exponential decrease with r, in correspondence with the Romanov−Solov'ev model of concentration fluctuations.[36−39] In that model, no spatial correlations of the fluctuating local concentration are taken into account. The $G(r)$ function for the solution of *N*,*N*′-$(Et)_2$U exhibits a relative maximum and indicates a broad distribution of relaxation times. The maxima occur, however, at rather small r values, which means that the relaxation times in the *N*,*N*′-$(Et)_2$U solutions are small, thus the fluctuation correlation lengths ξ (eq 9) are small. For the *N*-BuU solution, the relaxation-time distributions are again shifted to high values, indicating an increase in the fluctuation correlation length. At a solute concentration of 0.8 M, the $G(r)$ function resembles that of the *N*,*N*′-$(Et)_2$U solution. The shift, at increasing c, of the maximum in the relaxation-time distribution toward larger r is accompanied by a significant variation of the shape of the $G(\tau)$ function. This variation reflects the effect of the rate process. According to eq 12, it obviously short circuits the equilibration of the local concentrations by diffusion at long relaxation times τ_ξ (eq 7). Hence, if r approaches $\ln(\tau_o/\tau^*)$, the molecular dynamics is predominantly controlled by the rate process, offering a second pathway to the system to reach thermal equilibrium via local fluctuations in the distribution of the constituents. Obviously, in the *N*-BuU solutions with $c \geq 1$ M, fluctuations in the local concentration decay so slowly by diffusion that the parallel rate process becomes significant. According to the Kawasaki−Ferrell relation (eq 8), this includes the existence of noticeable fluctuation correlation lengths in these solutions.

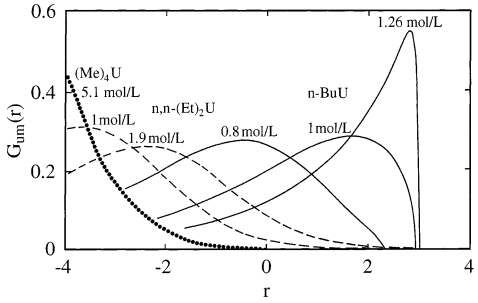

Figure 4. Relaxation-time distribution function $G_{um}(r)$ defined by eqs 14 and 15 for a solution of $(Me)_4U$ (· · ·), two *N*,*N*-$(Et)_2$U solutions (− − −), and three *N*-BuU solutions (—) in water at 25 °C.

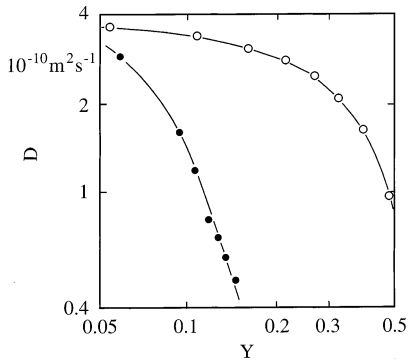

Figure 5. Mutual diffusion coefficient D vs mass fraction Y of solute for aqueous solutions of *N*-BuU (●) and tetra-*n*-butylammonium bromide[43] (○) at 25 °C.

Mutual Diffusion Coefficient. With each solute, the diffusion coefficients D obtained from the fitting procedure tend to decrease with solute concentration (Table 3). For the *N*-BuU solutions, this tendency is displayed in Figure 5, where the D values are shown along with those for tetrabutylammonium bromide (Bu_4NBr) solutions.[40] These aqueous solutions of organic ions also reveal indications of local concentration fluctuations. Their ultrasonic attenuation spectra have been evaluated consistently using D data in the fluctuation model that has been derived from the self-diffusion coefficients D_1 and D_2 of the solvent and the Bu_4N^+ ions, respectively. The relation[44]

$$D = (x_1D_1 + x_2D_2)(1 + (\partial \ln \gamma)/(\partial \ln x_2)) \qquad (16)$$

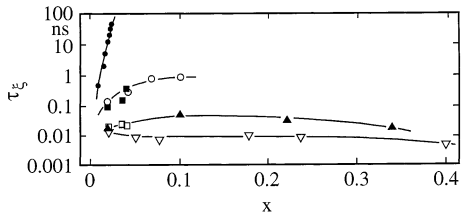

Figure 6. Decay time τ_ξ of concentration fluctuations vs mole fraction x of solute for aqueous solutions of EtU (▲), $(Me)_4U$ (▽), *N*,*N*-$(Et)_2U$ (□), *N*,*N*′-$(Et)_2U$ (■), and *N*-PrU (○).

has been used to calculate the mutual diffusion coefficient from *nmr* D_1 and D_2 data[45] and from the activity coefficient[46] γ of the aqueous Bu_4NBr solutions.

By analogy with the Stokes−Einstein equation, the Kawasaki−Ferrell relation (eq 8) suggests that local fluctuations in the concentration decay similarly to the diffusion of a spherical Brownian particle of radius ξ in a viscous medium with viscosity η_s. Therefore, the mutual diffusion coefficient is expected to decrease with solute concentration as the shear viscosity increases. The effect of shear viscosity is largely reflected by the diffusion coefficient from the Bu_4NBr solutions, the fluctuation correlation length of which is almost independent of concentration at $Y \geq 0.15$. The D values of the *N*-BuU solutions decrease more strongly with Y, pointing to a noticeable increase in the ξ values when approaching the limit of solubility of the urea derivative.

Decay Time and Fluctuation Correlation Length. By utilizing the (static) shear viscosity data η_s (Table 2), we have calculated the fluctuation correlation length ξ from the diffusion coefficients D. In addition, the decay times τ_ξ of concentration fluctuations

$$\tau_\xi = \xi^2/(2D) = (k_B T)^2/(72\pi^2\eta_s^2 D^3) \qquad (17)$$

can be calculated from η_s and D data using eq 8. Hence, τ_ξ and ξ are not independent of each another but may be alternatively used to point to different aspects of the same phenomenon.

In Figure 6, decay times τ_ξ of solutions of urea derivatives are shown as a function of mole fraction x. For $(Me)_4U$, EtU, and *N*,*N*-$(Et)_2U$, the τ_ξ values are almost independent of x and are on the order of 10 to 40 ps, corresponding with the time scale of molecular reorientations in those solutions.[47] Hence, there cannot exist noticeable fluctuations in the concentration. For solutions of *N*,*N*′-$(Et)_2U$ and the higher homologues *N*-PrU and *N*-BuU, significantly larger decay times emerge, indicating that the molecular motions of these systems are obviously dominated by concentration fluctuations. With these systems, τ_ξ increases with x and probably adopts a relative maximum that, for the *N*-PrU solutions, is located near $x = 0.07$ ($c = 3$ M). Relative maxima are revealed more clearly with aqueous solutions of other organic solutes with suitable hydrophilic/hydrophobic balance, such as alkohols and alkoxy alkanols.[40] There is a tendency for the mole fraction of the maximum τ_ξ value to decrease with increasing hydrophilic character of the solute. In Figure 7, we present the maximum ξ value for each urea derivative system along with data for alcohol/water and alkoxy alcohol/water mixtures. Within the series of unbranched molecules, the ξ_{max} data significantly increase with the length of the hydrophobic group of the solute. Surprisingly, the nature of the hydrophilic part of the organic solute is less important in determining the maximum correlation length ξ_{max}. We therefore conclude that the hydrophobic part of the organic molecules is important for the build up of more or less extended local

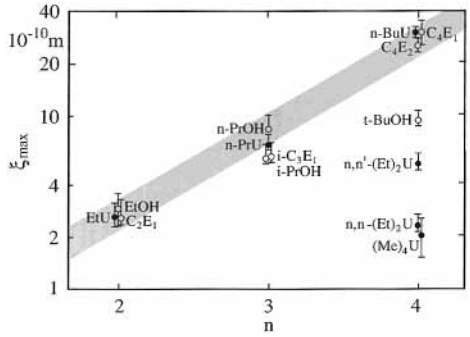

Figure 7. Maximum correlation length ξ_{max} for the concentration dependence of a solute/water system displayed as a function of the number n of $-CH_3$ and $-CH_2-$ groups per solute molecule for some urea derivatives, some monohydric alcohols, and some poly(ethylene glycol)monoalkyl ethers at 25 °C:[40] EtOH, ethanol; *n*- PrOH, *n*-propanol; *i*-PrOH, 2-propanol; *t*-BuOH, *tert*-butyl alcohol; C_2E_1, 2-butoxyethanol; $i\text{-}C_3E_1$, isopropoxyethanol; C_4E_1, 2-butoxyethanol; C_4E_2, 2-(2-butoxyethoxyl)ethanol.

fluctuations in the solute concentration. The more voluminous the (unbranched) hydrophobic part of the urea derivative is, the more pronounced is the tendency of the solute to avoid unfavorable effects of hydrophobic hydration. These effects can be reduced by the formation of clusters from solute molecules, by which water/solute interfaces are minimized. At the same time, hydrophobic interactions reduce the Gibbs free energy of the solution.

Clustering is much less marked with the isomers of *N*-BuU. Particularly with *N*,*N*-$(Et)_2U$ and $(Me)_4U$, the ξ_{max} values are on the order of molecular sizes, again indicating that in those systems effects from fluctuations in the local concentration do not exist.

Rate-Process Relaxation Time. The above view that hydrophobic hydration phenomena and hydrophobic interactions give rise to local fluctuations in the solute concentration implies equalization of concentration differences to proceed not only by diffusion but also by the rate process found in various spectra (Table 3). This process reflects a well-defined elementary reaction. Simulations have shown[48,49] that association due to hydrophobic interaction may be described by two distinguished configurations. In one configuration, a water layer exists between the hydrophobic groups; in the other configuration, the hydrophobic groups of different molecules are in direct contact with one another, surrounded by a common clathratelike hydration structure. Following Stillinger[50] and Endo,[42] we assume the relaxation with discrete relaxation time τ_o to couple to the reformation of clathratelike hydrophobic hydration regions, which is associated with the association and dissociation of solute clusters. For a dimerization process reaction scheme,

$$2A(H_2O)_m \underset{k_r}{\overset{k_f}{\rightleftharpoons}} A_2(H_2O)_n + (2m - n)H_2O \qquad (18)$$

describes the equilibrium between the hydrated monomers $A(H_2O)_m$ and dimers $A_2(H_2O)_n$. The relaxation rate of this equilibrium[30]

$$\tau_o^{-1} = k_f + k_r([A_2(H_2O)_n] + [(2m - n)H_2O]) \qquad (19)$$

is given by the forward and reverse rate constants k_f and k_r, respectively, and by the concentrations of the involved species.

In Figure 8, the relaxation times τ_o of the *N*-PrU and *N*-BuU solutions are displayed as a function of mole fraction of solute. Also shown for comparison are data for two series of solutions of alkoxy alkanols in water.[51] At low solute content, a tendency

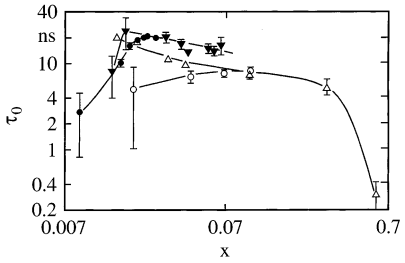

Figure 8. Relaxation time τ_o of the rate process in the fluctuation model (eq 12) vs mole fraction x of solute for aqueous solutions of *N*-PrU (▼), *N*-BuU(●), 2-butoxyethanol (○), and 2-(2-butoxyethoxy)-ethanol (△) at 25 °C. Curves are drawn to guide the eye.

of the τ_o values to increase with mole fraction x of solute is found. This is a reflection of the fact that the concentration of unaffected water $[(2m - n)H_2O]$ in eq 19 more strongly decreases with x than the concentration $[A_2(H_2O)_n]$ of hydrated dimers increases. The relaxation time τ_o reaches a relative maximum at a mole fraction at which the decrease in the concentration of the unaffected water just compensates for the increase in the concentration of the dimer complexes. At high x values, eq 19 is no longer valid because there is an insufficient amount of unaffected water left. The clathratelike hydration structures overlap. A clear distinction between two different configuations, separated by an enthalpy barrier, will fade. With decreasing height $\Delta H^{\#}$ of the enthalpy barrier, the relaxation time decreases.

In solutions of urea derivatives with small hydrocarbon groups, the enthalpy barrier $\Delta H^{\#}$ is smaller than in solutions of *N*-PrU and *N*-BuU, or it does not exist at all ($\Delta H^{\#} \ll RT$). Hence, there is no equilibrium between different configurations as defined by eq 18.

Amplitude Parameter. As briefly mentioned before, the amplitude parameter Q in the spectral function R_{um} of the unifying model of concentration fluctuations (eq 13) is given by the sum

$$Q = Q_{RS} + Q_{ML} \tag{20}$$

Herein, Q_{RS} denotes the Romanov−Solov'ev amplitude factor[36−39] given by the relation

$$Q_{RS} = \rho c_s^2 \frac{V^2 k_B T}{8\pi g^{||2}} \left(\frac{v^{||}}{V} - \frac{a_p}{c_p} h^{||} \right) \tag{21}$$

In this equation, V is the molar volume, a_p and c_p are the thermal expansion coefficient and heat capacity, respectively, at constant pressure, and the double primed quantities

$$g^{||} = \partial^2 G/\partial x^2 \qquad v^{||} = \partial^2 V/\partial x^2 \qquad h^{||} = \partial^2 H/\partial x^2 \tag{22}$$

are the second derivatives of the molar Gibbs free enthalpy, molar volume, and molar enthalpy, respectively, without contributions from fluctuations.

In Figure 9, the Q values of the solutions of urea derivatives are plotted versus the mole fraction x of solute. For solutions of EtU, *N*,*N*-$(Et)_2$U, *N*,*N*′-$(Et)_2$U, and $(Me)_4$U, the Q values are nearly constant. For solutions of *N*-PrU and *N*-BuU, however, for which significant fluctuation correlation lengths emerged, the amplitude factor significantly increased with x. Because $g^{||}$ of critical demixing systems vanishes when, within the one-phase region approaching the consolute point, we also assume the strong increase in the amplitude factor of the *N*-PrU and *N*-BuU systems to be due to very small $g^{||}$ values. Other

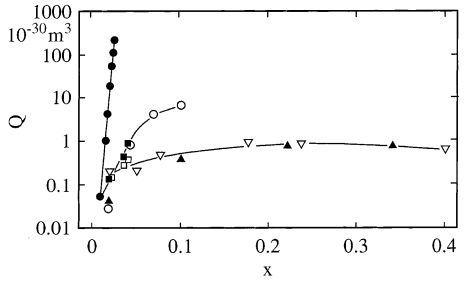

Figure 9. Amplitude parameters Q of the $R_{um}(\nu)$ function (eq 13) at 25 °C shown as a function of mole fraction x of solute for solutions of EtU (▲), $(Me)_4$U (▽), *N*,*N*-$(Et)_2$U (□), *N*,*N*′-$(Et)_2$U (■), *N*-PrU (○), and *N*-BuU (●) in water.

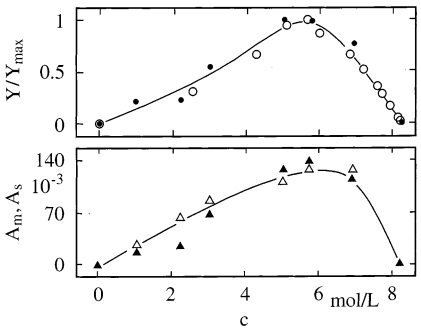

Figure 10. Amplitude parameter and shear viscosity ratio (●, $Y = Q$; ○, $Y = \eta_s$) as well as amplitudes $A_m = 2(\alpha\lambda)_{exc}(\hat{\nu})$ from the excess absorption spectra (▲) and A_s(△) from eq 26 for the $(Me)_4U/H_2O$ mixtures at 25 °C plotted vs tetramethylurea concentration c.

than with critical systems, the $g^{||}$ of solutions of urea derivatives does not vanish. Hence, these solutions display only noncritical concentration fluctuations.

For the solutions of EtU, *N*,*N*-*(Et)U*, *N*,*N*′-$(Et)_2$U, and $(Me)_4$U, the Q data do not show obvious effects from a decreasing second derivative of the Gibbs free energy. Rather, the amplitude factor seems to be dominated by the viscosity of the solutions, as illustrated for the tetramethylurea system in Figure 10. In that diagram, the Q data are compared to excess shear viscosity data defined by

$$\eta_{exc}(x) = \eta_s(x) - ((1 - x)\eta_s(0) + x\eta_s(1)) \tag{23}$$

Because Q and η_{exc} display a very similar dependence upon the mole fraction x of $(Me)_4$U, the comparison is an obvious attempt to relate the ultrasonic relaxation of tetramethylurea/water mixtures to a shear viscosity relaxation. Assuming a Debye-type relaxation with discrete relaxation time τ_s and with relaxation strength

$$\Delta\eta_s = \lim_{\nu \to 0}(\eta_s(\nu)) - \lim_{\nu \to \infty}(\eta_s(\nu)) \tag{24}$$

a (Debye) relaxation with relaxation amplitude

$$A_s = \frac{4\pi}{3} \frac{1}{\rho c_s^2} \frac{\Delta\eta_s}{\tau_s} \tag{25}$$

follows in the ultrasonic absorption per wavelength. The nice agreement of the amplitude values from eq 25 with those from the experimental spectra of $(Me)_4$U solutions (Figure 10) may be taken to indicate a close relation of the ultrasonic excess absorption to a viscosity relaxation. Hence, the Q_{ML} contribution seems to dominate the amplitude factor (eq 20) of the $(Me)_4U$/water mixture. For the EtU, *N*,*N*-$(Et)_2$U, and *N*,*N*′-$(Et)_2$U

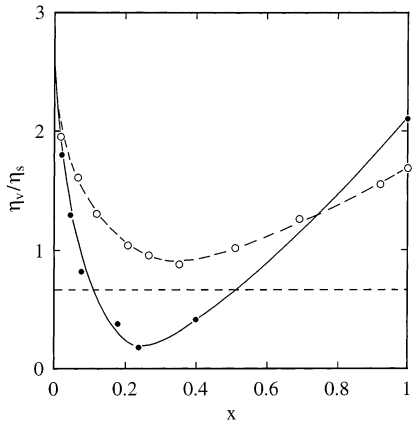

Figure 11. Volume/shear viscosity ratio vs mole fraction x of the nonaqueous constituent for mixtures of $(Me)_4U$ (●) and dimethyl sulfoxide[53] (○) with water (25 °C).

solutions, we do not know the excess viscosities because these urea derivatives are solid at room temperature. Estimations using $\eta_{exc} = \eta_s$ show that the effect of a shear viscosity relaxation decreases with the length of the alkyl group (e.g., from $(Me)_4U$ to *N*-BuU solutions). For the *N*-BuU solutions at concentrations above 1 M, only 1 to 10% of the ultrasonic relaxation amplitude is estimated to be due to a relaxation of η_s.

Volume Viscosity to Shear Viscosity Ratio. For nonmetallic liquids, contributions from the nonvanishing heat conduction to the asymptotic high-frequency absorption per wavelength can be neglected. The *B* parameter (eq 4) in the ultrasonic spectra thus reflects viscosity contributions and excess absorption contributions with a relaxation frequency well above our measuring range. The viscosity contributions are given by[52]

$$B = \frac{8\pi^2}{3\rho c_s^2}\left(\eta_s - \frac{3}{4}\eta_\nu\right) \tag{26}$$

where η_ν denotes the volume viscosity which is related to the curl-free part of the acoustical field. Because we measured the (static) shear viscosities of the solutions (Table 2), the *B* data (Table 3) can be evaluated to yield the volume-viscosity/shear-viscosity ratio η_ν/η_s. In Figure 11, this ratio is displayed as function of mole fraction x for the $(CH_3)_4U/H_2O$ system and also for mixtures of dimethyl sulfoxide (DMSO) and water.[53] The high value for the viscosity ratio of water ($\eta_\nu/\eta_s = 2.68$) is assigned to the bulky hydrogen-bonded structure of water at room temperature, which is assumed to be subject to a relaxation with a frequency of approximately 100 GHz.[52,54] Obviously, this structure is successively destroyed upon addition of solutes. At $x < 0.3$, $d(\eta_\nu/\eta_s)/dx < 0$ is also found with the other series of solutions of urea derivatives in water. For the $(CH_3)_4U/H_2O$ and $DMSO/H_2O$ systems, the η_ν/η_s data adopt a relative minimum near $x = 0.3$ to reach rather high values again at $x = 1$: $\eta_\nu/\eta_s = 2.1$ for $(CH_3)_4U$, and $\eta_\nu/\eta_s = 1.7$ for DMSO. Both liquids are aprotic, so a hydrogen-bonded liquid structure cannot be the reason for the high volume-viscosity/shear-viscosity ratio. It has been suggested that DMSO molecules associate.[53] An indication for association, for instance, is the shear viscosity of DMSO ($\eta_s = 1.96 \times 10^{-3}$Pa s, 25 °C), which is much higher than that of similarly structured acetone ($\eta_s = 0.3 \times 10^{-3}$Pa s, 25 °C). The static (electric) permittivity of DMSO ($\epsilon(0) = 47.0 \pm 0.6$, 25 °C) has been discussed[55] in terms of antiparallel ordering of the molecular electric dipole moments $\vec{\mu}$ ($\mu = |\vec{\mu}| = 3.91$D[56]). It is possible that some similar associations also occur in tetramethylurea. If the relaxation frequency corresponding to the autocorrelation time of such non-hydrogen-bonded associated structures is above our measuring range, then fluctuations of the structures will contribute to the asymptotic high-frequency absorption coefficient. In addition, $(Me)_4U$ might exist in two conformations that differ from each another by the orientation of the $-N(CH_3)_2$ groups.

If no special structure features exist, $\eta_\nu/\eta_s = {}^2/_3$ is predicted to be the minimum viscosity ratio of the liquids.[57,58] Some $(Me)_4U/H_2O$ mixtures (Figure 11) and some aqueous solutions of EtU exhibit viscosity ratios noticeably smaller than 0.67. Such small η_ν/η_s values (<0.67) have also been found with aqueous solutions of alkoxy alkanols. One reason for this finding could be a dispersion in the shear viscosity, which was not taken into account when calculating the η_ν/η_s data. A shear viscosity relaxation has been reported recently for some monohydric alcohols[59] and is thus not unlikely to exist within our frequency range of measurements or in the solutions of urea derivatives.

5. Conclusions

Up to very high solute concentrations, no ultrasonic excess absorption has been found in the acoustical spectra that could be attributed to either of the reaction schemes that had been proposed previously in order to account for the unique properties of aqueous urea solutions. Depending on the hydrocarbon groups, alkyl derivatives of urea, however, tend to associate when dissolved in water. The ultrasonic excess absorption spectrum reflecting such association processes can be well represented by the unifying model of concentration fluctuations. This model is based on a particular spatial correlation of fluctuations, considering short range correlations with a nearly exponential decay function and long-range correlations with Ornstein−Zernike behavior. Also taken into account is a rate process that proceeds parallel to the local concentration fluctuations. It is assumed to reflect a dimerization mediated by hydrophobic interactions. The correlation length of the local fluctuations in concentration and the relaxation rate of these fluctuations are strongly correlated with the hydrophobic properties of the solute. The fluctuation correlation length increases with the length of the (unbranched) alkyl group. It decreases significantly if the hydrocarbon groups are distributed instead of being concentrated in one unbranched alkyl chain.

Acknowledgment. Financial assistance by the Deutsche Forschungsgemeinschaft, Bonn, Germany, is gratefully acknowledged.

References and Notes

(1) Franks, F.; Reid, D. S. In *Water in Crystalline Hydrates; Aqueous Solutions of Simple Nonelectrolytes;* Franks, F., Ed.; Water: A Comprehensive Treatise; Plenum: New York, 1973; Vol. 2, Chapter 5.
(2) Stokes, R. H. *Aust. J. Chem* **1967**, *20*, 2087.
(3) Frank, H. S.; Franks, F. *J. Chem. Phys.* **1968**, *48*, 4746.
(4) Hammes, G. G.; Schimmel, P. R. *J. Am. Chem. Soc.* **1966**, *89*, 442.
(5) Beauregard, D. V.; Barrett, R. E. *J. Chem. Phys.* **1968**, *49*, 5241.
(6) Bödecker, G. Diploma-Thesis, Georg-August-Universität, Göttingen, Germany, 1974.
(7) Finer, E. G.; Franks, F.; Tait, M. J. *J. Am. Chem. Soc.* **1972**, *94*, 4424.
(8) Walrafen, G. E. *J. Chem. Phys.* **1966**, *44*, 3726.
(9) Pottel, R.; Adolph, D.; Kaatze, U. *Ber. Bunsen-Ges. Phys. Chem.* **1975**, *79*, 278.
(10) Petong, P.; Pottel, R.; Kaatze, U. *J. Phys. Chem. A* **2000**, *104*, 7420.
(11) Schwerdtfeger, S.; Köhler, F.; Pottel, R.; Kaatze, U. *J. Chem. Phys.* **2001**, *115*, 4186.
(12) Tanaka, H.; Ohmine, I. *J. Chem. Phys.* **1987**, *87*, 6128.
(13) Ohmine, I.; Tanaka, H.; Wolynes, P. G. *J. Chem. Phys.* **1988**, *89*, 5852.
(14) Sciortino, F.; Fornili, S. L. *J. Chem. Phys.* **1989**, *90*, 2786.

(15) Sciortino, F.; Geiger, A.; Stanley, H. E. *J. Chem. Phys.* **1992**, *96*, 3857.
(16) Ohmine, I.; Tanaka, H. *Chem. Rev.* **1993**, *93*, 2545.
(17) Kaatze, U.; Pottel, R. *J. Mol. Liq.* **1992**, *52*, 181.
(18) Kaatze, U.; Behrends, R.; Pottel, R. *J. Non-Cryst. Solids*, in press.
(19) Blandamer, M. J. In *Acoustic Properties;* Franks, F., Ed.; Water: A Comprehensive Treatise; Plenum: New York, 1973; Vol. 2, Chapter 9.
(20) Eggers, F.; Kaatze, U. *Meas. Sci. Technol.* **1996**, *7*, 1.
(21) Kaatze, U.; Behrends, R.; Lautscham, K. *Ultrasonics* **2001**, *39*, 393.
(22) Eggers, F.; Kaatze U.; Richmann, K. H.; Telgmann, T. *Meas. Sci. Technol.* **1994**, *5*, 1131.
(23) Kaatze, U.; Wehrmann, B.; Pottel, R. *J. Phys. E: Sci. Instrum.* **1987**, *20*, 125.
(24) Kononenko, V. S. *Sov. Phys. Acoust.* **1985**, *31*, 499.
(25) Kaatze, U.; Kühnel, V.; Menzel, K.; Schwerdtfeger, S. *Meas. Sci. Technol*. **1993**, *4*, 1257.
(26) Kaatze, U.; Lautscham, K.; Brai, M. *J. Phys. E: Sci. Instrum.* **1988**, *21*, 98.
(27) Kaatze, U.; Kühnel, V.; Weiss, G. *Ultrasonics* **1996**, *34*, 51.
(28) Bömmel, H. E.; Dransfeld, K. *Phys. Rev. Lett.* **1958**, *1*, 234.
(29) Kaatze, U.; Lautscham, K. *J. Phys. E: Sci. Instrum.* **1986**, *19*, 1046.
(30) Strehlow, H. *Rapid Reactions in Solution*; VCH: Weinheim, Germany, 1992.
(31) Anisinov, M. A. *Critical Phenomena in Liquids and Liquid Crystals*; Gordon and Breach: Philadelphia, PA, 1991.
(32) Ornstein, L. S.; Zernike, F. *Phys. Z.* **1918**, *19*, 134.
(33) Ornstein, L. S.; Zernike, F. *Phys. Z.* **1926**, *27*, 763.
(34) Kawasaki, K. *Ann. Phys. (N. Y.)* **1970**, *61*, 1.
(35) Ferrell, R. A. *Phys. Rev. Lett.* **1970**, *24* 1969.
(36) Romanov, V. P.; Solov'ev V. A. *Sov. Phys. Acoust.* **1965**, *11*, 68.
(37) Romanov, V. P.; Solov'ev, V. A. *Sov. Phys. Acoust.* **1965**, *11*, 219.
(38) Romanov, V. P.; Solov'ev, V. A. In *Water in Biological Systems*; Vuks, M. F., Sidrova, A. J., Eds.; Consultant Bureaus: New York, 1971; Vol. 2, p 1.
(39) Romanov, V. P.; Ul'yanov, S. V. *Physica A* **1993**, *201*, 527.
(40) Rupprecht, A.; Kaatze, U. *J. Phys. Chem. A* **1999** *103*, 6485.
(41) Montrose, C. J.; Litovitz, T. A. *J. Acoust. Soc. Am.* **1979**, *47*, 1250.
(42) Endo, H. *J. Chem. Phys.* **1990**, *92*, 1986.
(43) Kühnel, V.; Kaatze, U. *J. Phys. Chem.* **1996**, *100*, 19747.
(44) Crank, J.; Park, G. S. *Diffusion in Polymers*; Academic Press: London, 1968.
(45) Hertz, H. G.; Lindman, B.; Siepe, V. *Ber. Bunsen-Ges. Phys. Chem.* **1969**, *73*, 542.
(46) Lindenbaum, S.; Boyd, G. E. *J. Phys. Chem.* **1964**, *68*, 911.
(47) Kaatze, U.; Gerke, H.; Pottel, R. *J. Phys. Chem.* **1986**, *90*, 5464.
(48) Pangali, C.; Rao, M.; Berne, B. J. *J. Chem. Phys.* **1979**, *71*, 2975.
(49) Ben-Naim, A. *Hydrophobic Interactions*; Plenum Press: New York, 1980.
(50) Stillinger, F. H. *Science (Washington, D.C.)* **1980**, *209*, 4455.
(51) Menzel, K.; Rupprecht, A.; Kaatze, U. *J. Phys. Chem. B* **1997**, *101*, 1255.
(52) Davis, C. M.; Jarzynski, J. In *Water: A Comprehensive Treatise*; Franks, F., Ed.; Plenum Press: New York, 1972; Vol. 1, p 443.
(53) Kaatze, U.; Brai, M.; Scholle, F.-D.; Pottel, R. *J. Mol. Liq.* **1990**, *44*, 197.
(54) Litovitz, T. A.; Davis, C. M. In *Physical Acoustics*; Mason, W. P., Ed.; Academic Press: New York, 1965; Vol. 2A, p 281.
(55) Kaatze, U.; Pottel, R.; Schäfer, M. *J. Phys. Chem.* **1989**, *93*, 5623.
(56) *Digest of Literature on Dielectrics;* Wertheimer, M. R.; Yelon, A., Eds.; National Academy of Sciences: Washington, DC, 1979; Vol. 41, p 57.
(57) Madigosky, W. M.; Warfield, R. W. *J. Chem. Phys.* **1983**, *78*, 1912.
(58) Madigosky, W. M.; Warfield, R. W. *Acustica* **1984**, *55*, 123.
(59) Behrends, R.; Kaatze, U. *J. Phys. Chem. A* **2001**, *105*, 5829.